Lawrence Berkeley National Laboratory
Recent Work

Title
APPLICATIONS OF SURFACE TECHNIQUES TO CHEMICAL BONDING STUDIES OF MINERALS

Permalink
https://escholarship.org/uc/item/62p1861d

Author
Perry, D.L.

Publication Date
1986-03-01

Lawrence Berkeley Laboratory
UNIVERSITY OF CALIFORNIA

EARTH SCIENCES DIVISION

To be published as a chapter in Chemical
Reactions at the Mineral/Water Interface,
J.A. Davis and K.F. Hayes, Eds., American
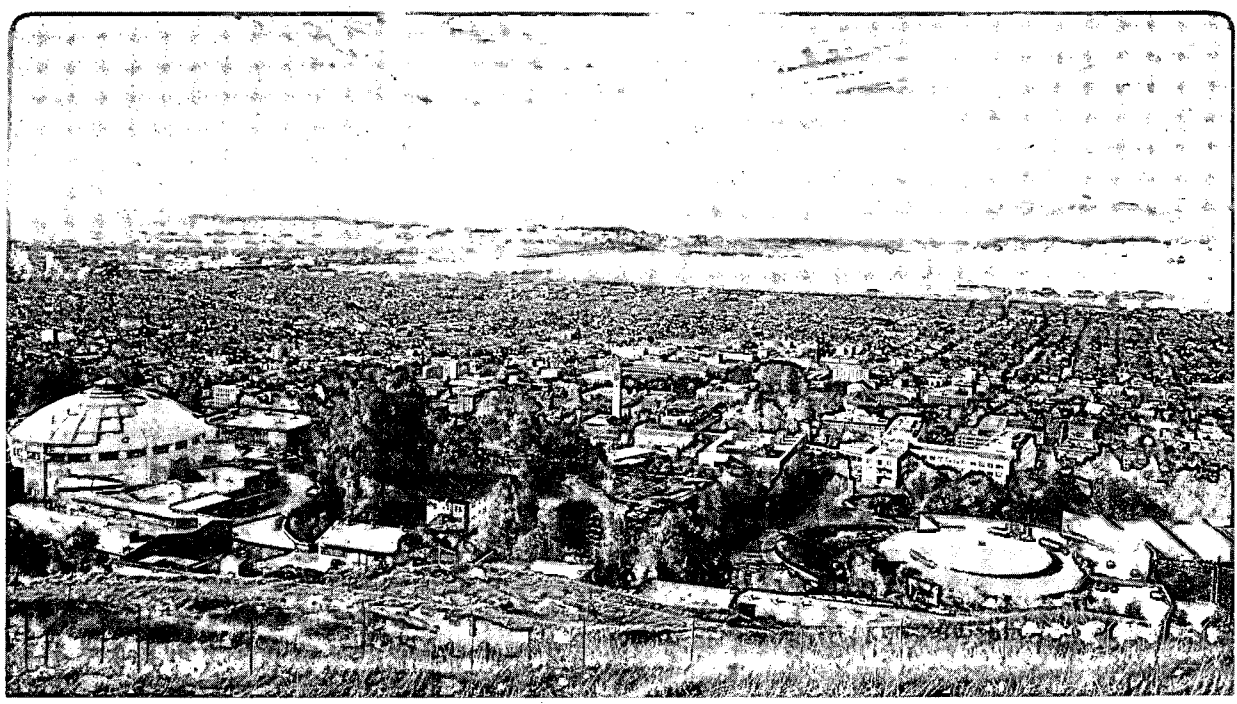Chemical Society, Washington, DC, 1986

APPLICATIONS OF SURFACE TECHNIQUES TO
CHEMICAL BONDING STUDIES OF MINERALS

D.L. Perry

March 1986

DISCLAIMER

Applications of Surface Techniques to Chemical Bonding Studies of Minerals

Dale L. Perry

Lawrence Berkeley Laboratory
University of California
Berkeley, CA 94720

Applications of Surface Techniques to Chemical
Bonding Studies of Minerals

Dale L. Perry

Lawrence Berkeley Laboratory .
University of California
Berkeley, CA 94720

In the last several years, a number of new instrumental techniques have been
developed that are quite effective in detecting changes in the surfaces of minerals
that have undergone chemically induced reactions or natural geologic alterations.
These techniques are able to yield a large amount of information concerning the
chemical bonding of both the mineral itself and any surface species that are
present. The present paper addresses x-ray photoelectron, Auger, and combined
x-ray photoelectron/Auger spectroscopy (including the Auger parameter concept)
and discusses many of the important spectral parameters associated with them
that are useful for determining the chemical states of elements found in mineral
systems. Problems related to the vacuum-oriented techniques — such as dehydra-
tion, charging, and metal ion reduction — are discussed, along with methods of
studying samples as a function of depth. Examples of applications of these con-
cepts to studies of bonding in minerals and related surface species are discussed.

During the last several years, a number of new instrumental surface techniques have been
developed that are quite effective in detecting changes in the surfaces of minerals that have
undergone chemically induced or natural geologic alteration. These techniques are quite sen-
sitive (approximately 0.1–0.5% atomic concentration for x-ray photoelectron and Auger spec-
troscopy, for example), and they make it possible to monitor very small amounts of elements
that may be present in the near surface material. Any change in the surface with respect to
chemical composition may readily be measured qualitatively and, in some cases, quantita-
tively. As a result, this type of research in surface science is merely another application to
reaction systems involving aqueous solution/solid interfaces: many other areas of research,
such as aqueous corrosion (1) and electrochemistry (2), have used surface science almost since
its inception.

Surface measurements as part of a geochemical study have several advantages.
First, the techniques collectively are sensitive to all elements in the periodic table, although
hydrogen and helium cannot be detected by x-ray photoelectron and Auger spectroscopy (two
of the most widely used techniques). Second, several of the techniques, such as x-ray pho-
toelectron spectroscopy, give important information about the chemical bonding environment
of the element being studied. Third, surface studies involve only the first several layers of the
substrate, where mineral-solution interactions have their greatest effect. Finally, many sur-
face methods can be coupled with depth profiling to actually measure changes in elemental
concentration as a function of depth below the surface layer of minerals.

Even though the vacuum-oriented surface techniques yield much useful

information about the chemistry of a surface, their use is not totally without problems. Hydrated surfaces, for example, are susceptible to dehydration due to the vacuum and localized sample heating induced by x-ray and electron beams. Still, successful studies have been conducted on aquated inorganic salts (*3*), water on metals (*3*), and hydrated iron oxide minerals (*4*). Even aqueous solutions themselves have been studied by x-ray photoelectron spectroscopy (*5*). The reader should also remember that even dry samples can sometimes undergo deterioration under the proper circumstances. In most cases, however, alterations in the sample surface can be detected by monitoring the spectra as a function of time of x-ray or electron beam exposure and by a careful, visual inspection of the sample.

Another problem that can be encountered in x-ray photoelectron (and Auger) spectroscopy is that of charging. This problem arises from the fact that many samples under study are not in electrical equilibrium. This equilibrium can be attained only if an electron flow from ground can be achieved to neutralize the residual positive charge on the sample surface created by the photoemission process. For those minerals that are insulators, the conductivity may not be sufficient to prevent a positive charge from building on the surface; this results in a false increase in the binding energy. There are several ways of addressing charging, including the use of low energy electrons to neutralize the positive charge (*6*), gold decoration of the sample (*7*), and the contaminant carbon 1s line (*8*). This problem has been reviewed by several authors (*9,10*), as has been the Auger parameter concept discussed below, which circumvents this problem.

Metal ion reduction can also occur during surface studies. One of the best documented examples is that of the reduction of copper(II) to copper(I), a process that has been reviewed extensively in the research literature (*11*). Certain copper(II) minerals, such as CuO (tenorite), are quite susceptible to photoreduction (*11*), and care must be taken in conducting surface studies on them. Uranium(VI) salts chemisorbed on zeolites have also been observed (*12*) to undergo photoreduction to uranium(IV) compounds. Mechanisms for photoreduction of CuO, for example, have been widely reported in the chemical research literature (*13-17*).

Keeping these problems in mind, several of the more widely used techniques are discussed below, with an emphasis placed on their application to bonding studies of minerals and species adsorbed on them during mineral/water interface reactions. As with *any* experimental techniques, many of these problems can be minimized or even eliminated if due caution is taken in performing the studies.

X-Ray Photoelectron Spectroscopy (XPS)

X-ray photoelectron spectroscopy (also called electron spectroscopy for chemical analysis, or ESCA) is a surface technique that can be used to detect elements qualitatively (and quantitatively, in some cases) in the surface layers of solids, as well as the chemical states (species) of the elements. The basic experimental apparatus for performing XPS studies includes an x-ray source (most commonly, Mg Kα or Al Kα radiation), an electron energy analyzer, a specimen holder, and a vacuum chamber. As the x-rays impinge on the solid samples, electrons are emitted from the surface. The electron energy analyzer then measures the kinetic energy of the emitted electrons, which can be related directly to the binding energy of the electron in that particular atom. The binding energies of the individual atoms yield much information about their chemical states.

X-ray photoelectron spectroscopy can be performed on any sample that is vacuum compatible, i.e., does not decompose under vacuum in the range $10^{-7} - 10^{-10}$ torr. In most cases, the technique does little or no damage to the sample surface, although x-ray-induced chemical reactions such as those discussed above may occur. As a surface technique, it gives a signal that mirrors approximately the top 15 to 40 of the surface (*18*).

The following aspects of x-ray photoelectron spectroscopy are important in terms of determining bonding both in chemical species on minerals and in the minerals themselves. Data obtained from these spectral parameters are both structural and electronic, and, when

considered with crystallographic structural data where possible, give a comprehensive bonding picture. Of course, for general survey treatises of this technique, prior works (*19–21*) should be consulted.

Binding Energy. The most often cited spectral parameter in x-ray photoelectron spectroscopy is the binding energy. Not only do photoelectron lines indicate a particular element, but they also represent a chemical state (or species) of that element. The core photoelectron lines of many elements are quite sensitive to the electronic state of that element from two standpoints: oxidation state and the functional group of which the element is a component. In some cases, the differences in binding energies for various oxidation states are quite large, e.g., Cr(III) vs. Cr(VI), Fe(II) vs. Fe(III). In other cases, the binding energy separation between oxidation states is not so large as to differentiate unequivocally between them, e.g., Cu(I) vs. Cu(0), Co(II) vs. Co(III). The distinction between the members of the latter sets of ions must be made on the basis of other spectroscopic parameters, such as multiplet splitting, satellite structure, and spin-orbit splitting (discussed below). The same is also true when one is trying to differentiate among members of a series of similar compounds (e.g., different oxides of a metal in the same oxidation state).

Figure 1, for example, shows a survey scan of natural galena, PbS. Besides lead and sulfur, one also sees the oxygen inherent in natural samples and the chlorine resulting from groundwater fluid inclusions; all are nicely separated in terms of their binding energies. But if one looks at a high resolution spectrum of the fused sulfur $2p_{3/2,1/2}$ line (Figure 2), it is seen that there are several sulfur species present. The sulfide form, part of the galena itself, is observed at 160.4 eV, while the elemental sulfur and sulfate forms are found at 163.8 and 168.3 eV, respectively (*22*). In some weathered galena samples, the thiosulfate ion ($S_2O_3^{2-}$) can also be detected (*23*); this ion has additional line components in both the sulfide and sulfate region due to the presence of two states of sulfur in that ion. In this case, the different forms of the sulfur can be quite easily differentiated on the basis of the marked differences in the binding energies and line shapes. Figure 3 shows a similar situation for the sulfur 2p spectra of chalcocite and covellite, two naturally occurring copper(I) minerals (*24*). The sulfide region of the spectrum of covellite is more complex, since it contains both S^{2-} (sulfide) and S_2^{2-} (disulfide) ions; chalcocite contains only the simple sulfide ion. In these cases, the line shapes (the contour of the photoelectron peak of an element) are also quite different.

Satellite Structure. Another experimental parameter obtained from x-ray photoelectron spectra is that of satellites. These lines, which can be either weak or strong relative to the main photoelectron line with which they are associated, appear to the high binding energy side of that photoelectron line. They result from coupled electronic processes brought about by the initial ionization of an atom in the emission of the photoelectron. These satellites can arise from several different types of these processes. When the kinetic energy of the primary ejected electron is "shared" with valence electrons to promote another electron to an excited state, the resulting satellite is referred to as a "shake-up" satellite; when this "sharing" results in another electron being promoted to a continuum state, the result is a "shake-off" satellite. These satellites vary in their position relative to the main peak as a function of the chemical state of the element being studied. For extensive treatises on these satellites, the reader should consult more comprehensive review articles (*25–27*).

Figure 4 is a good example of satellite structure associated with a surface species. The chromium $2p_{3/2,1/2}$ spectrum results from the reaction of the dichromate ion, $Cr_2O_7^{2-}$, with galena to yield both chromium(VI) (indicated by an asymmetric, broadened shoulder on the high binding energy side of the main chromium(III) peak) and a reduced chromium(III) species. The satellite located 10.3 eV to the high binding energy side of the chromium(III) line (the main $2p_{1/2}$ line at 586.4 eV) has been shown (*28*) to be a mixed chromium(III) oxide-carbonate complex. The chromium(VI) species,

which is diamagnetic and thus yields no significant satellite structure, was identified as $PbCrO_4$.

Spin-Orbit Splitting. When ionization of a p, d, or f orbital occurs to produce a photoelectron, one of the results is a phenomenon referred to as spin-orbit splitting. This ionization (*19-21*) yields two ionic states and thus two major peaks. If one again looks at Figure 3, he can see the copper 2p photoelectron line split into the $2p_{3/2}$ and $2p_{1/2}$ components; the same doublet also is observed for the chromium 2p line in Figure 4, where the splitting is 9.6 eV for the chromium(VI) species and 9.4 eV for the chromium(III) species. The magnitude of the splitting is many times a function of the oxidation state of the element being studied, such as in the case of chromium. It is sometimes associated with the differences in ligands or the coordination sphere of the central element, although the difference in splitting is rather minimal for these two latter cases. It is usually greatest for elements that exhibit differences in oxidation state along with differences in electronic spin state; for example, diamagnetic cobalt(III) exhibits a spin-orbit splitting much different from that of paramagnetic, "high-spin" cobalt(II) (*15*).

Multiplet Splitting. Photoionization in a core shell coupled with one or more valence shell electrons results in multiplet splitting, a phenomenon (*25*) that can be utilized to study paramagnetic systems. The effects of multiplet splitting may manifest themselves in a variety of ways. In the case of 3d ions, such as those found in the first row transition elements, the 2p photoelectron lines undergo broadening. The copper $2p_{3/2,1/2}$ lines shown in Figure 3 would be considerably broader if the copper species being observed were the paramagnetic, $3d^9$ copper(II) system. Also, the 3s photoelectron lines of the 3d block of transition elements actually undergo a splitting into a doublet for paramagnetic ions. By careful study of the 3s photoelectron level, in conjunction with good chemical standards, one can learn much about the bonding of species on a reacted mineral surface or about the substrate itself.

Taken as a whole, then, the above spectroscopic parameters — binding energy, satellite structure, spin-orbit and multiplet splitting, and line shapes — give a more comprehensive picture of the chemistry of a surface. If one looks at the entire set of data (Table I) pertaining to the spectrum shown in Figure 4, he can see that the chromium(III) species on the galena surface is hydrated chromium(III) oxide with a reaction layer film of CO_2 that has formed a mixed hydrated oxide/carbonate complex (*28*). Both "$Cr(OH)_3$" and "$Cr_2(CO_3)_3 \cdot nH_2O$" are reaction products of the reaction of hydrated chromium(III) oxide and CO_2; the chief difference is that the "$Cr(OH)_3$" will contain less carbonate material, resulting in a smaller spin-orbit splitting than "$Cr_2(CO_3)_3 \cdot nH_2O$" (*28*).

Auger Electron Spectroscopy (AES)

Auger electron spectroscopy (*29*) is a type of electron spectroscopy that is used for determining solid surface elemental and electronic composition. An experiment is conducted by bombarding a solid surface with an electron beam of energy ranging from 1 keV to 10 keV. Alternatively, an x-ray source can be used. The Auger electrons, emitted from an atom by means of a radiationless transition, are

5

Table I. X-Ray Photoelectron Data for the Galena/$Cr_2O_7^{2-}$
Reaction and Related Cr(III) Compounds[a,b]

Sample	Cr $2p_{3/2}$	Cr $2p_{1/2}$	O 1s	C 1s[c]
Galena/$Cr_2O_7^{2-}$	577.0–Cr(III)	586.4–Cr(III)	530.9	288.0
	578.8–Cr(VI)	588.4–Cr(VI)		
Cr_2O_3	576.3	586.1	529.9	
$Cr(OH)_3$[e]	576.6	586.4	530.8	288.0
$Cr_2(CO_3)_3 \cdot nH_2O$[f]	577.0	587.1	531.2	288.0

Sample	Cr $(2p_{1/2}-2p_{3/2})$	Cr 3s Splitting	Cr $2p_{1/2}$ Satellite[d]
Galena/$Cr_2O_7^{2-}$	9.4-Cr(III)	4.1–4.3	10.3
	9.6-Cr(VI)		
Cr_2O_3	9.8	4.3	10.3
$Cr(OH)_3$[e]	9.8	4.1	10.3
$Cr_2(CO_3)_3 \cdot nH_2O$[f]	10.1	4.1	10.3

[a]All values in electron volts, eV.

[b]Adventitious (contaminant) carbon 1s = 284.6 eV.

[c]Carbon line attributable to the carbonate species.

[d]Distance (to the high binding energy side) from the main $2p_{1/2}$ line.

[e]Also formulated as $Cr_2O_3 \cdot nH_2O \cdot xCO_2$; please see text.

[f]Also formulated as $Cr_2O_3 \cdot nH_2O \cdot xCO_2$; please see text.

detected by an energy analyzer. The sensitivity of this technique is a function of the probability of the Auger transition peculiar to a particular element, the current and energy of the impinging electron or x-ray beam, and the efficiency of the electron analyzer.

The Auger effect is based on the following processes. Upon ionization of a core atomic level in a solid sample, the atom may undergo a decay to a lower energy level. This leaves the atom in a doubly ionized state, and the energy difference between the two states is transmitted to the ejected Auger electron. Those Auger transitions that occur near the surface of the solid result in ejected Auger electrons that do not undergo electron energy loss. The shape and energy of the resulting Auger peaks are thus useful in identifying the elemental composition of the sample surface as well as obtaining useful chemical information.

While historically many Auger data have been obtained using an electron beam to generate the Auger spectra in the form of derivative (or dN/dE vs. electron binding energy) spectra, the spectra can be recorded also in the counting mode (or N(E)/E vs. electron binding energy, the format used in Figure 1). This spectral representation allows the researcher to study spectral line shapes for elements that many times have much more detailed features than they would exhibit in the derivative mode. Two additional advantages of x-ray-induced Auger electron spectroscopy are that surface charging is much less of a problem for geologic materials (most of which are insulators), and surface damage is generally less for samples

irradiated under x-ray beams than for the same samples irradiated by an electron beam. Auger spectroscopy can also be used in a scanning mode (scanning Auger microscopy, or SAM) to yield surface topographical and elemental distribution data (*30*).

Figure 5 gives a good illustration of high resolution x-ray-induced Auger electron spectra for lead oxide minerals and related intermediates and products arising from their oxidation and thermal decomposition reactions (*31*). One can readily see, for example, that the oxygen KVV spectrum of the yellow form of PbO (the mineral massicot), shown in Figure 5a, is quite different from that of PbO_2 (plattnerite), shown in Figure 5d; the kinetic energies of the oxygen KVV Auger lines are also quite different.

"Combined X-Ray

As mentioned above, an Auger spectrum also can be generated by an appropriate x-ray source such as Al $K\alpha$ or Mg $K\alpha$, which are used to generate x-ray photoelectron spectra; one result is shown in Figure 1. Not only are photoelectron lines such as the lead 4f, 4d, and 5d lines present, but one also sees oxygen and carbon Auger lines. High resolution studies of these Auger lines, coupled with the x-ray photoelectron lines in the same spectrum, allow a more complete and detailed study of the chemical and electronic states of the elements present.

One chief advantage of having both the x-ray photoelectron and Auger spectra combined is that a researcher can make use of *Auger parameters*. Auger parameters (*32–34*) are a concept by which use is made of both x-ray photoelectron lines and the x-ray-induced Auger lines to characterize a chemical species. The approach has two major advantages. First, chemical shifts in x-ray-excited Auger lines are usually larger and very different from those observed for the photoelectron lines; this is quite important in terms of being better able to identify a particular compound. Secondly, since the positions of the Auger line and photoelectron line are relative to one another in the same spectrum, the uncertainty in spectral line position due to charging no longer exists. In effect, the Auger parameter provides an internal reference value for each compound of a particular element. In the ideal case, this value will be a unique one and will be sufficiently different from those of other compounds to differentiate it unequivocally. Unfortunately, Auger parameters of several compounds or techniques may be very close to one another, and the use of other parameters may be necessary to identify them spectroscopically.

While the Auger parameter can be expressed in several ways, one of the most commonly used definitions is that shown in Equation 1

$$\alpha' = BE_{photo} + KE_{Auger} \qquad (1)$$

where α' is the modified Auger parameter, BE_{photo} is the charge-corrected binding energy of the photoelectron line for the element studied, and KE_{Auger} is the charge-corrected kinetic energy of an appropriate Auger line for the same element. In choosing which photoelectron and Auger lines are used to compute the Auger parameter, the deciding factors are the sharpness and intensity of the lines as well as their sensitivities to changes in the differences in the bonding environment of the element studied.

Table II shows representative Auger parameters for several silicon and aluminum species. Both mineral and non-mineral species are shown to give some idea of the range of values. For these calculations, the fused silicon and aluminum $2p_{3/2,1/2}$ photoelectron lines are used in conjunction with the KLL Auger lines.

After one considers the experimental aspects of combined x-ray photoelectron/Auger spectroscopy discussed above, he can then use the data in Table III to differentiate between the minerals chalcocite (Cu_2S) and covellite (CuS) (Fig. 3). Differences are in the sulfur $2p_{3/2,1/2}$ binding energies and the kinetic energies of the copper LVV observed Auger lines. Additionally, the line shape and peak width differences of the sulfur $2p_{3/2,1/2}$ spectra, coupled with the differences between the copper $2p_{3/2}$ and sulfur $2p_{3/2}$

binding energies (a full electron volt), allow the investigator to differentiate between the two minerals spectroscopically. Again, all of the spectral parameters *as a whole* must be taken together to obtain the best results in distinguishing between the two sulfides.

Table II. Representative Auger Parameters
for Silicon and Aluminum[a,b]

Silicon	$2p_{3/2,1/2}$	$KL_{23}L_{23}$	α'
α-cristobalite, SiO_2	103.2	1608.6	1711.8
α' -quartz, SiO_2	103.6	1608.6	1712.2
Vycor, SiO_2	103.5	1608.5	1712.0
Si_3N_4	101.9	1612.2	1714.1
Si	99.6	1616.3	1715.9
Aluminum	**$2p$**	**$KL_{23}L_{23}$**	**α'**
Boehmite, AlO(OH)	74.2	1387.6	1461.8
Bayerite, $Al(OH)_3$	74.3	1387.7	1462.0
Gibbsite, $Al(OH)_3$	74.0	1387.4	1461.4
AlAs	73.6	1391.2	1464.8
AlN	74.0	1388.9	1462.9
Al	72.9	1393.2	1466.1

[a]Abstracted from Wagner, C.D., In "Practical Surface Analysis by Auger and X-Ray Photoelectron Spectroscopy"; Briggs, D. and Seah, M.P., Eds.; John Wiley and Sons, Ltd.: New York, 1983; Appendix 4, p. 477.
[b]In electron volts, eV.

Table III. X-Ray Photoelectron and Auger Data for
Chalcocite and Covellite[a,b]

	S $2p_{3/2}$	Cu $2p_{3/2}$	Cu $2p_{1/2}$	Cu L_3VV[c]	α^{*}[d]	Δ[e]
Cu_2S	161.7(2.2)	932.6(1.9)	952.3(2.3)	917.3	1849.9	770.9
CuS	162.5(2.8)	932.4(1.9)	952.2(2.3)	917.9	1850.3	769.9

[a]All spectra referenced to C 1s at 285.0 eV.

[b]Numbers in parentheses next to the copper and sulfur 2p binding
energies represent the full width at half maximum (FWHM) of those
photoelectron lines.

[c]Kinetic energies for the Auger lines were determined from their
apparent binding energies (KE = hν-BE).

[d]Modified Auger parameter for copper.

[e]The differences in binding energies between the Cu $2p_{3/2}$ and
S $2p_{3/2}$ photoelectron lines.

In addition to studying an "as received" mineral sample surface, the researcher
can also study samples as a function of the depth into the bulk by means of depth profiling
studies. This can be performed in two ways: ion sputtering and electron grazing angle
analysis. In ion sputtering, rare gas (usually argon) ions are used to remove layers of the sam-
ple surface. This approach is a destructive technique and can totally alter the chemistry of
the surface that existed before sputtering; functional groups such as carbonates, sulfates, and
nitrates are usually destroyed by sputtering. Also, sputtering affects the contaminant carbon
1s peak, thus causing some uncertainty in using this line for charge compensation. Another
problem observed for this technique is that of differential elemental sputtering: different ele-
ments sputter at different rates. All of these problems have been discussed extensively in
review articles (*35,36*).

Electron grazing angle analysis takes advantage of the increase of surface sensi-
tivity in x-ray photoelectron spectroscopy by using variations in grazing angle of electron
emission from the surface sample. For optimum results, the sample surface should be without
irregularity or roughness, since changes in the surface contour can severely affect the surface
sensitivity as a function of the electron emission angle. Still, this technique has the chief
advantage of being non-destructive; this allows depth profiling without disturbing the initial
surface chemistry of the sample surface. This approach has been reviewed by several investi-
gators (*37*).

The above techniques have a wide array of applications, including those that are
both analytical and physicochemical (such as bonding) in nature. Typical examples of
research include the surface chemistry of ferrite minerals (*38*) and the valence states of copper
in a wide array of copper (*39*) minerals. Other areas of bonding that have been studied
include the oxidation state of vanadium (*40*) in vanadium-bearing aegirines (also using x-ray
photoelectron spectroscopy) and the surface features of titanium perovskites (*41*).

Other areas of geologic research that can be explored using a combined instrumen-
tation approach are many. Surface reactions of solids that have been suspended in aqueous
solutions can be studied; this type of work has important applications in mineral processing
research. The analysis of precious and strategic metal ores can be studied in order to monitor
their inherent material and chemical properties and their surface characteristics before and
after reaction.

In summary, any mineral solid surface that is involved in a geologic process (either

natural or laboratory induced) or reaction can be studied from a standpoint of the bonding and chemistry of the surface as well as from an analytical standpoint. As a result of this approach, more valuable information can be obtained about the mineral surface than if the mere analytical approach is used exclusively. The additional information regarding the surface is useful for predicting reaction stoichiometries, mechanisms, and rates that are pertinent to aqueous geochemical processes.
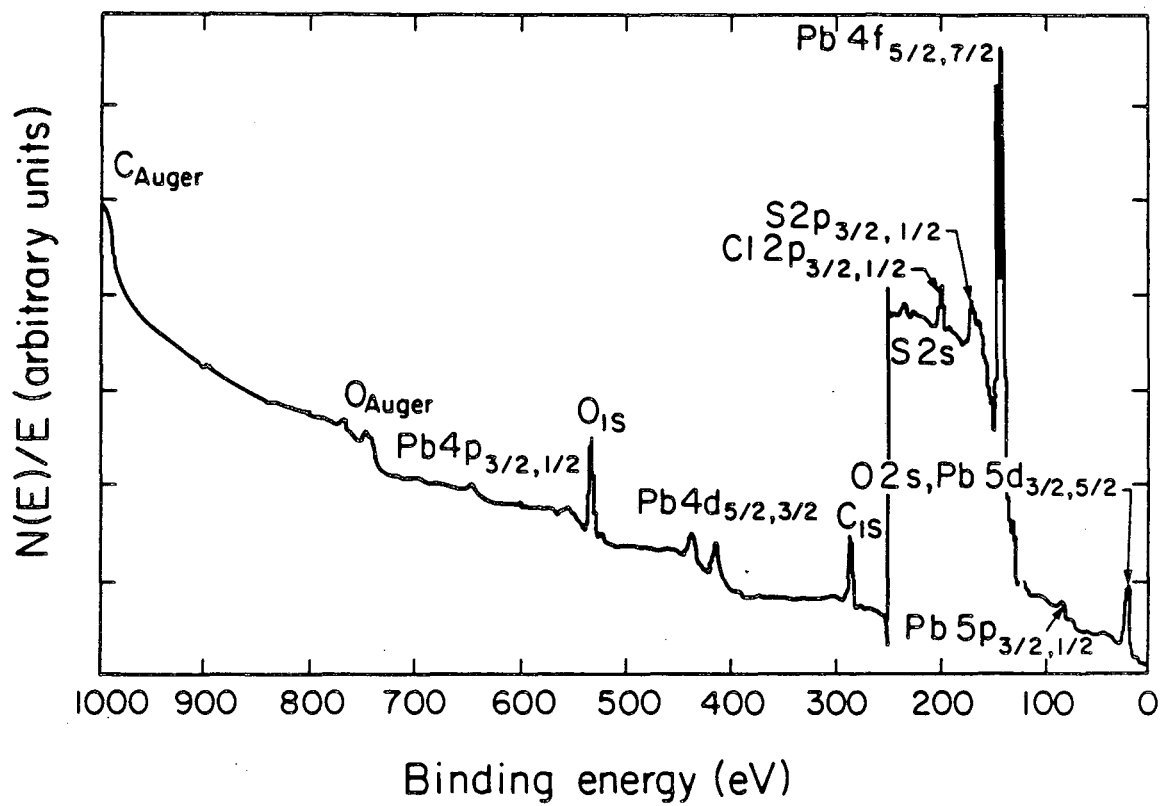
Acknowledgments

Literature Cited

1. Baer, D.R.; Thomas, M.T. In "ACS Symposium Series, No. 199, Industrial Applications of Surface Analysis," L.A. Casper and C.J. Power, Eds., American Chemical Society: Washington, D.C., 1982.
2. Sherwood, P.M.A. *Chem. Soc. Rev.* 1985, 14, 1–44.
3. Hirokawa, K.; Danzaki, Y. *Surf. Interface Anal.* 1982, 4, 63–7.
4. McIntyre, N.S.; Zetaruk, D.G. *Anal. Chem.* 1977, 19, 1521–29.
5. Avanzino, S.C.; Jolly, W.L. *Inorg. Chem.* 1978, 100, 2228–30.
6. Lewis, R.T.; Kelly, M.A. *J. Electron Spectrosc. Relat. Phenom.* 1980, 20, 105–115.
7. Hnatowich, D.J.; Hudis, J.; Perlman, M.L.; Ragaini, R.C. *J. Appl. Phys.* 1971, 42, 4883.
8. Swift, P. *Surf. Interface Anal.* 1982, 4, 47–51.
9. Broughton, J.Q.; Perry, D.L. *Surf. Sci.* 1978, 74, 307–17.
10. Reference 8 and references therein.
11. Klein, J.C.; Li, C.P.; Hercules, D.M.; Black, J.F. *Appl. Spectrosc.* 1984, 38, 729–34.
12. Perry, D.L.; Suib, S., unpublished data.
13. Wallbank, B.; Johnson, C.E.; Main, I.G. *J. Electron Spectrosc. Relat. Phenom.* 1974, 4, 263–69.
14. Rosencwaig, A.; Wertheim, G.K. *J. Electron Spectrosc. Relat. Phenom.* 1972/73, 1, 493–96.
15. Frost, D.C.; Ishitani, A.; McDowell, C.A. *Mol. Phys.* 1972, 24, 861–77.
16. Hirokawa, K.; Honda, F.; Oku, M. *J. Electron Spectrosc. Relat. Phenom.* 1975, 6, 333–45.
17. Sarma, D.D. *Indian J. Chem.* 1980, 19, 1046–49.
18. Klasson, M.; Hedman, J.; Berndtsson, A.; Nilsson, R.; Nordling, C. *Physica Scripta* 1972, 5, 93–5.
19. Siegbahn, K.; Nordling, C.N.; Fahlman, A.; Nordberg, R.; Hamrin, K.; Hedman, J.; Johansson, G.; Bergmark, T.; Karlsson, S.E.; Lindgren, I.; and Lindberg, B. "ESCA, Atomic, Molecular, and Solid State Structure Studied by Means of Electron Spectroscopy"; Almqvist and Wiksells: Upsala, 1967.
20. Siegbahn, K.; Nordling, C.; Johansson, G.; Hedman, J.; Heden, P.F.; Hamrin, K.; Gelius, U.; Bergmark, T.; Werme, L.O.; Manne, R.; and Baer, Y. "ESCA Applied to Free Molecules"; North-Holland: Amsterdam, 1969.
21. Jolly, W.L. *Coord. Chem. Rev.* 1974, 13, 47–81.
22. Lindberg, B.J. *Int. J. Sulfur Chem. C* 1972, 7, 33–52.
23. Lindberg, B.J.; Hamrin, K.; Johansson, G.; Gelins, U.; Fahlmann, A.; Nordling, C.; Siegbahn, K. *Phys. Scr.* 1970, 1, 297–309.
24. Perry, D.L.; Taylor, J.A. *J. Mat. Sci. Lett.*, in press.
25. Vernon, G.A.; Stucky, G.; Carlson, T.A. *Inorg. Chem.* 1976, 15, 278–84.
26. Brisk, M.A.; Baker, A.D. *J. Electron Spectrosc. Related Phenom.* 1975, 7, 197–213.

27. Aarons, L.J.; Guest, M.F.; Hillier, I.H. *J. Chem. Soc., Faraday Trans. II* 1972, 68, 1866–74.

28. Perry, D.L.; Tsao, L.; Taylor, J.A. *Inorg. Chim. Acta* 1984, 85, L57–L60.

29. Thompson, M.; Baker, M.D.; Cristie, A.; Tyson, J.F. "Auger Electron Spectroscopy"; Wiley-Interscience: New York, 1985.

30. Prutton, M. *Scanning Electron Microsc.* 1982, 1, 83–91.

31. Taylor, J.A.; Perry, D.L. *J. Vac. Sci. Technol. A* 1984, 2, 771–4.

32. Wagner, C.D.; Gale, L.H.; Raymond, R.H. *Anal. Chem.* 1979, 51, 466–82.

33. Wagner, C.D. In "Practical Surface Analysis by Auger and X-Ray Photoelectron Spectroscopy"; D. Briggs, and M.P. Seah Eds.; John Wiley and Sons, Ltd.: New York, 1983; Appendix 4, p. 477.

34. Wagner, C.D.; Passoja, D.E.; Hillery, H.F.; Kinisky, T.G.; Six, H.A.; Jansen, W.T.; Taylor, J.A. *J. Vac. Sci. Technol.* 1982, 21, 933–44.

35. Coyle, G.J.; Tsang, T.; Adler, I.; Ben-Zvi, N. *J. Electron Spectrosc. Related Phenom.* 1981, 24, 221–36.

36. Hofman, S. *Surf. Interface Anal.* 1980, 2, 148–60.

37. Ebel, M.F. *J. Electron Spectrosc. Relat. Phenom.* 1978, 14, 287–322.

38. Perry, D.L.; Bonnell, D.W.; Parks, G.D.; Margrave, J.L. *High Temp. Sci.* 1977, 9, 85–98.

39. Nakai, I.; Sugitani, Y.; Nagasimi, K.; Niwa, Y. *J. Inorg. Nucl. Chem.* 1978, 40, 789–91.

40. Nakai, I.; Ogawa, H.; Sugitani, Y.; Niwa, Y.; Nagashima, K. *Mineral. J.* 1976, 8, 129–34.

41. Myhra, S.; Bishop, H. E.; Riviere, J. C. *Surf. Technol.* 1983, 19, 161-72.
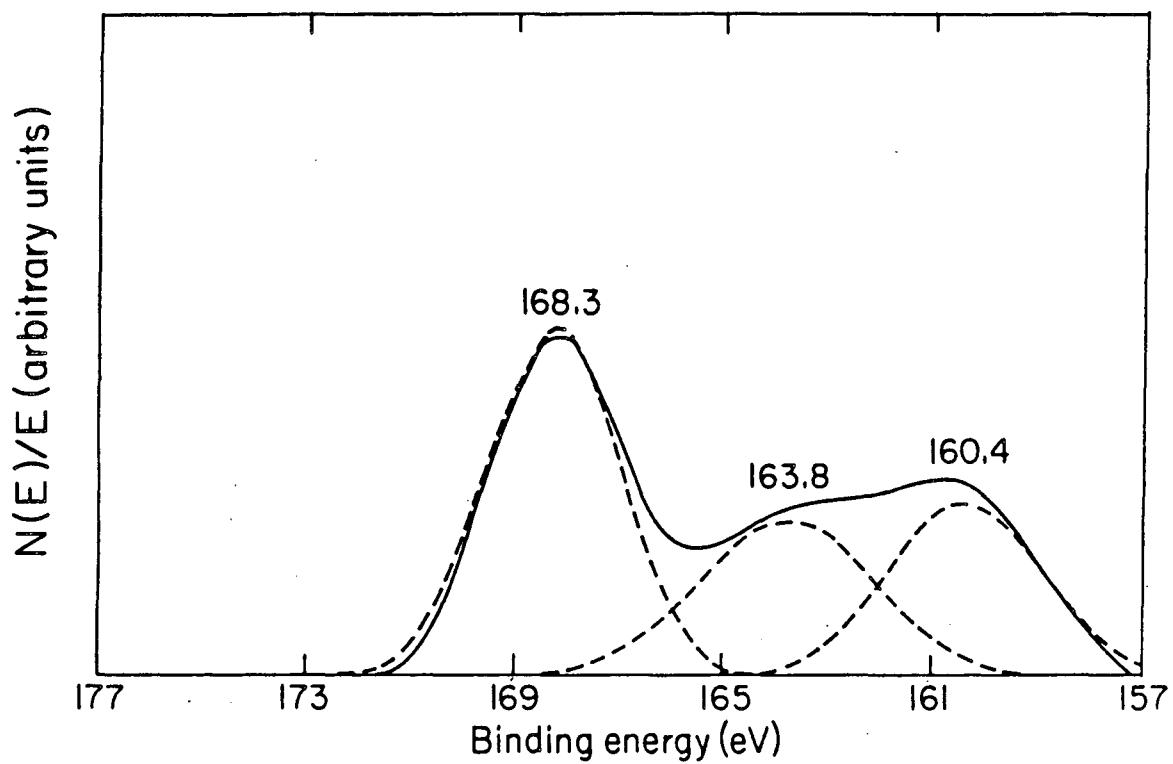
Figure Captions

Figure 1.   X-ray photoelectron survey scan of naturally weathered galena, PbS.

Figure 2.   High resolution x-ray photoelectron spectrum of naturally weathered galena, PbS, in the sulfur $2p_{3/2,1/2}$ region.

Figure 3.   The copper $2p_{3/2,1/2}$ and sulfur $2p_{3/2,1/2}$ x-ray photoelectron spectra of natural chalcocite (Cu_2S) and covellite (CuS).

Figure 4.   The chromium $2p_{3/2,1/2}$ photoelectron spectrum of galena that has been reacted with an aqueous solution of $Na_2Cr_2O_7$. The broken vertical lines through the main peaks indicate the photoelectron peaks associated with the chromium(VI) species, while the solid vertical lines indicate the photoelectron lines associated with the chromium(III) species.

Figure 5.   The 0 KVV Auger and 0 1s photoelectron lines for (a) powdered yellow PbO (massicot) as received, (b) same sample heated *in situ* in O_2, (c) clean metallic lead exposed to 500 L of O_2 at 150 ° C, (d) powered PbO_2 (plattnerite) as received, (e) same sample heated to 320 ° C *in vacuo*, (f) powdered Pb_3O_4 (minium) and (g) powdered $2PbCO_3 \cdot Pb(OH)_2$ (hydrocerussite).
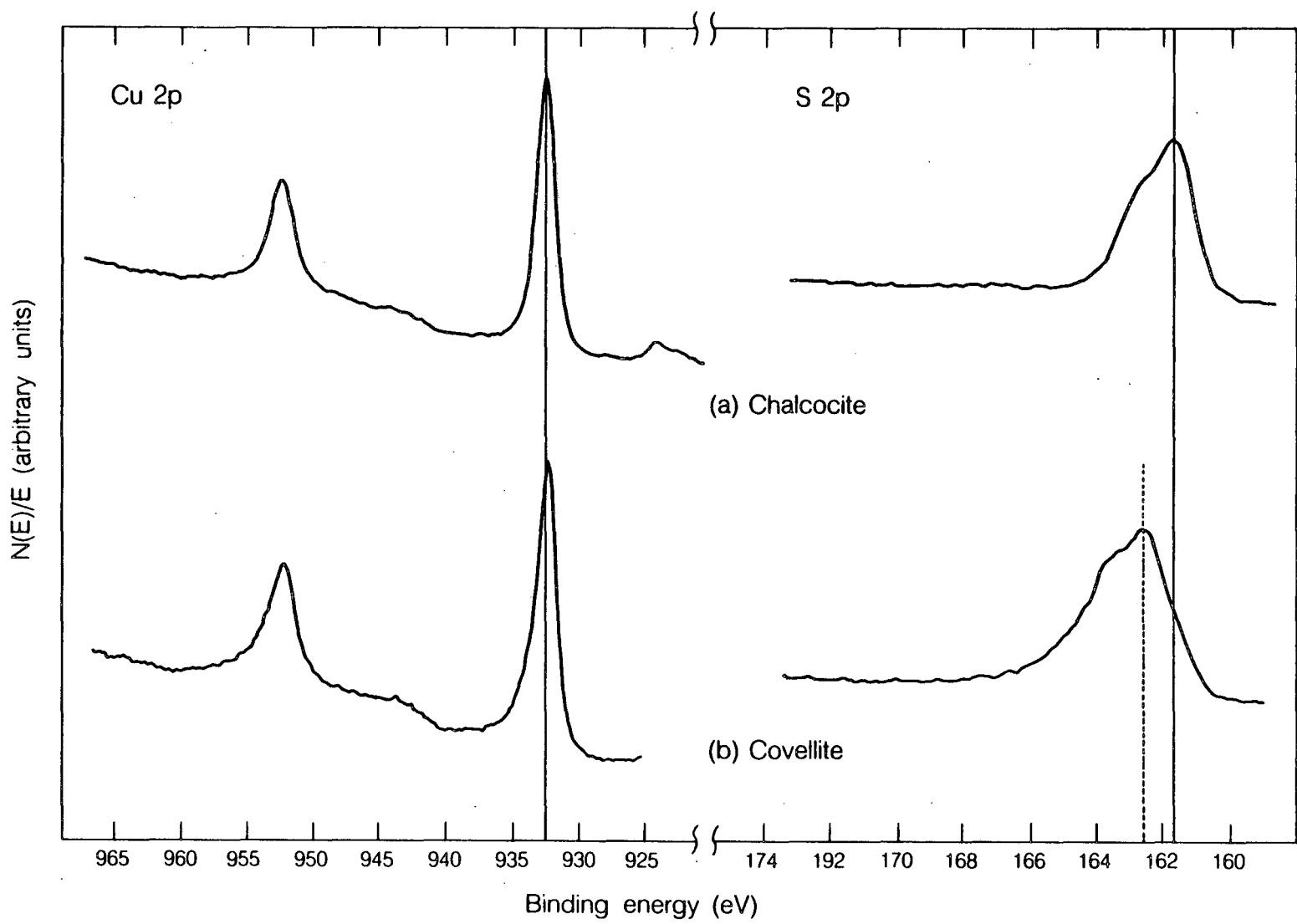
Fig. 1.

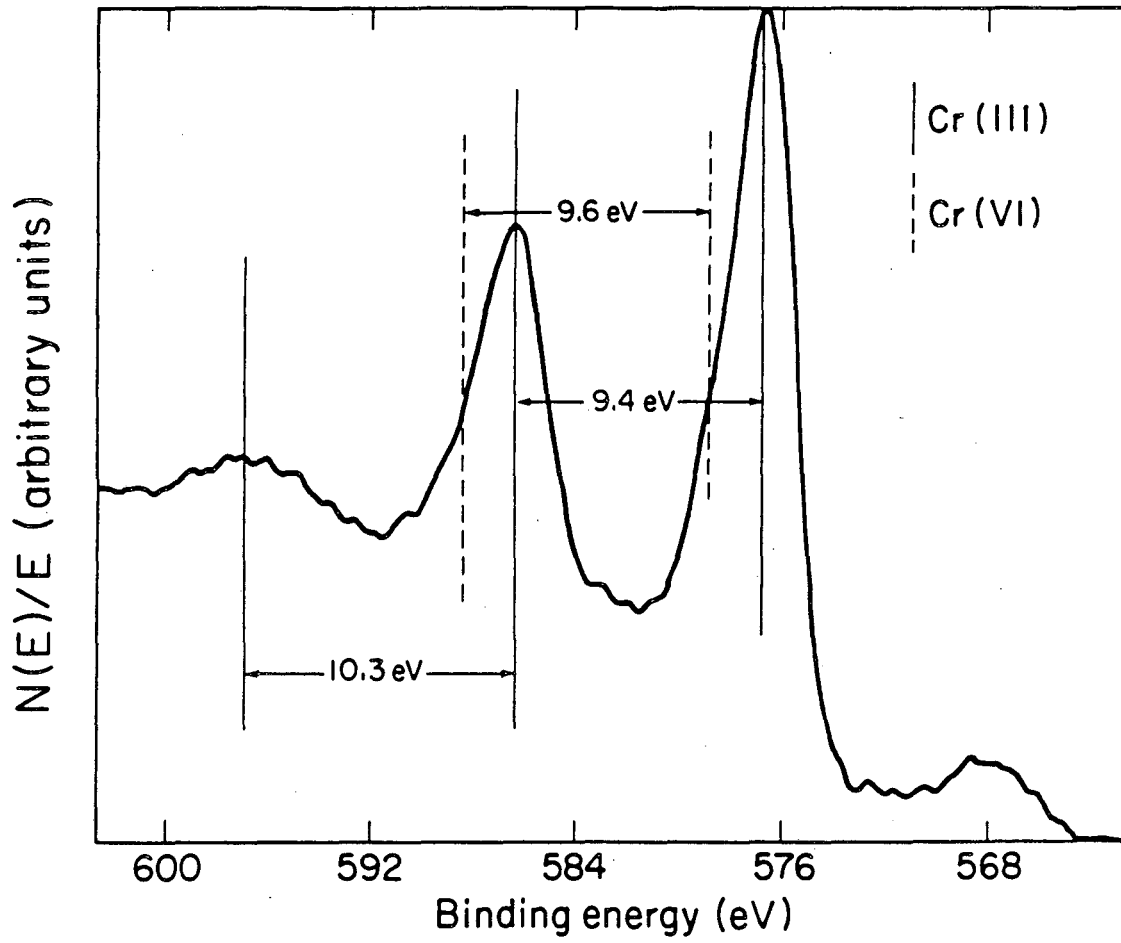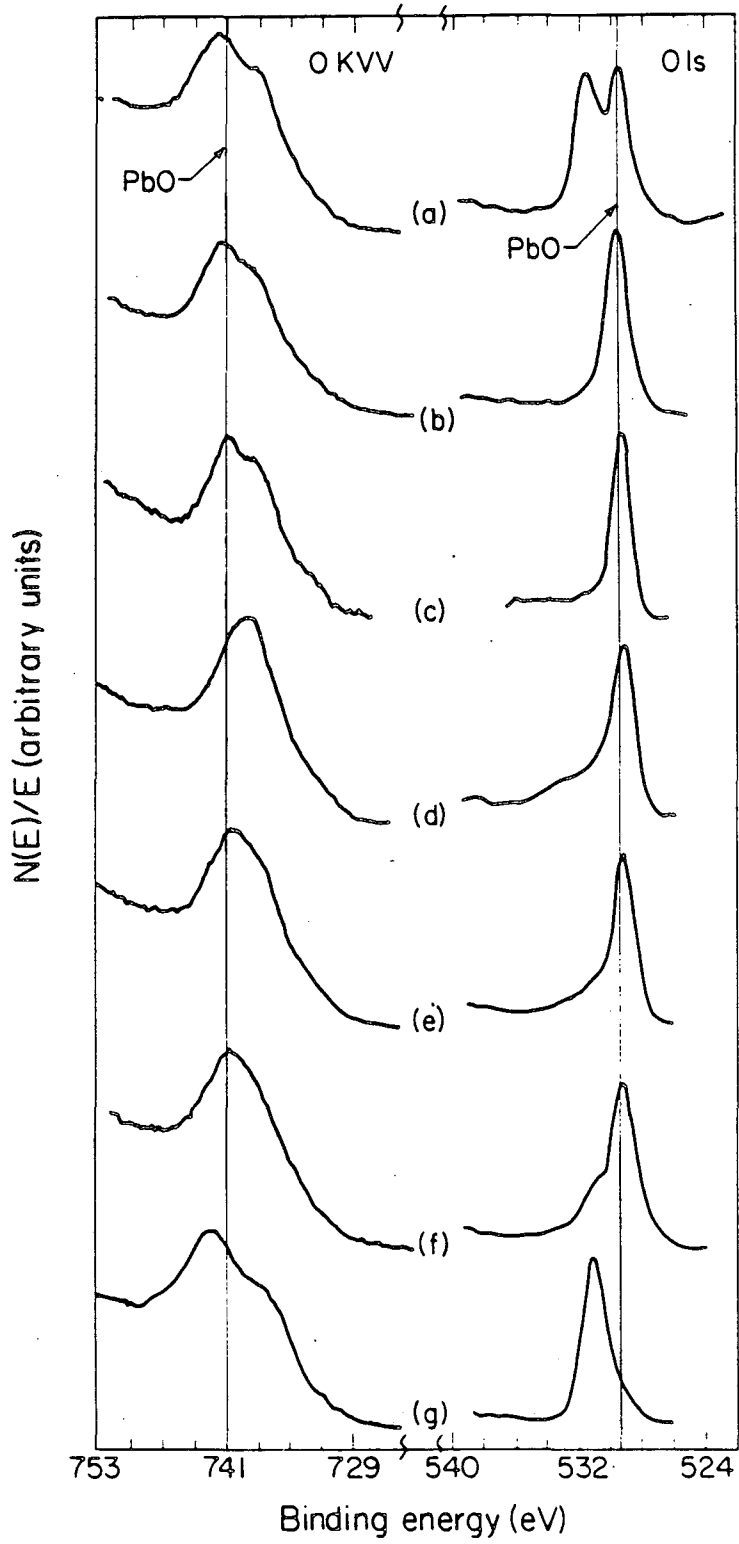Binding energy (eV)

XBL 859-10686

XBL 8210-2580

Cu 2p

S 2p

(a) Chalcocite

(b) Covellite

N(E)/E (arbitrary units)

965 960 955 950 945 940 935 930 925   174 192 170 168 166 164 162 160

Binding energy (eV)

14

Fig. 3.

XBL 846-8955

Fig. 4.

Fig. 5.

N(E)/E (arbitrary units)

Binding energy (eV)

753   741   729   540   532   524

O KVV

O ls

PbO

PbO

(a)
(b)
(c)
(d)
(e)
(f)
(g)

XBL 833-1392